

## Coordinated System for Real Time Muscle Deformation during Locomotion

**Sandra Baldassarri**

(University of Zaragoza, Spain  
sandra@unizar.es)

**Francisco Seron**

(University of Zaragoza, Spain  
seron@unizar.es)

**Abstract:** This paper presents a system that simulates, in real time, the volumetric deformation of muscles during human locomotion. We propose a two-layered motion model. The requirements of realism and real time computation lead to a hybrid locomotion system that uses a skeleton as first layer. The muscles, represented by an anatomical surface model, constitute the second layer, whose deformations are simulated with a finite element method (FEM). The FEM subsystem is fed by the torques and forces got from the locomotion system, through a line of action model, and takes into account the geometry and material properties of the muscles. High level parameters (like height, weight, physical constitution, step frequency, step length or speed) allow to customize the individuals and the locomotion and therefore, the deformation of the persons' muscles.

**Key Words:** Animation, Muscle Deformation, Human Locomotion, Finite Element Method

**Category:** I.3, I.6, G.1.10

### 1 Introduction

Realistic modeling and animation of the human body have been widely analyzed in many fields including computer graphics, computer vision or biomechanics. However, these areas still remain as important challenges due to the complexity of representing the appearance of the human body (consisting in rigid parts and soft tissues) and, most important, due to our familiarity with human shape and human movement.

The approaches to simulate the animation of the body are usually based on the movement of the underlying skeleton. The segments that constitute the skeleton are enough to represent individuals when different movements are considered. However, the description of the body shape must be taken into account when representing some other characteristics like weight, age or physical constitution. To achieve this, it's necessary that a muscular layer is superimposed to the skeleton.

The system presented here is a step towards the automatic simulation of the deformation of the lower limb muscles during locomotion, based in a two-layered

model. A hybrid dynamics-kinematics locomotion system is used to determine the orientation and displacement of the body segments. The pattern of the forces that act over the muscles is obtained by a *line of action model* inserted in the skeletal model. The line of action model is used to estimate the force of a specific group of muscles, and this resultant force is used as a boundary condition in a linear *Finite Element Model (FEM)* to generate the deformation of each individual muscle or group of muscles. This system is specially interesting for adding naturalness to virtual humans in virtual reality environments, video games or in applications in which real time restrictions make impossible to achieve a precise and exceptional visual quality.

Unlike other works, our systems allows to customize the locomotion and the muscle deformation for different individuals and to solve the following problems:

- How can be represented persons walking with the same speed but with different weights?
- How does it change the trajectory of the center of mass of the body if the step length varies?
- How does the quadriceps of a person of 1.80 mts, 80 kg and athletic constitution deform when he walks at 5 km/h? And with a specific step length or step frequency?
- What's the difference if the person is taller o thinner?

After this introduction, the paper is organized as follows. Section 2 gives an overview of the related research. Section 3 presents a general description of our approach. Sections 4 and 5 describe, respectively, the different phases that conforms the system: the skeletal phase that produces the body motion simulation and the musculoskeletal phase that includes the computation of the forces acting in the muscles and their consequent deformation. Section 6 exposes some of our experimental results, and finally, Section 7 presents the conclusions of the paper.

## 2 Related Work

Basically, the process of animating virtual humans involves two stages: the description of the body shape and the generation of the body movement. However, the body shape changes during the animation. So, to represent the complexity of the human body is essential to tackle the simulation of the muscles and the deformations caused by the movement of the skeleton.

Many research work has been made independently in the different areas related with our investigation: human body modeling and animation [Duf07]

[WSS<sup>+</sup>09], human motion: from gait analysis [Mur67] [Whi03] [SPL<sup>+</sup>05] to human motion capture [MG06] [Per01] [MHK01] and muscle deformation: either from a biomechanical point of view [VTT<sup>+</sup>06] [BR08] or for interactive applications [ZCK98] [LGK<sup>+</sup>09] [CSC10]. However, in this paper we focus **only** on those approaches in which there is a direct relation between the body motion and the muscle deformation.

One of the firsts works in the simulation of muscle deformation was presented by Chen y Zeltzer [CZ92]. They simulate the contraction of single muscles with a Finite Element Method (FEM) but they don't achieve real time animation.

Since then, several works use different approaches for modeling and simulating muscle deformation [LGK<sup>+</sup>09].

One of the most used approaches consist in using simplified musculoskeletal models. In some works, the muscle bellies are represented by deformable ellipsoids and the shape of the muscle is recalculated each time the joint origin or insertion moves [Wil95] [Wil97] [SPCM97]. Komura *et al.* use generalized cylinders for representing the muscles, and the deformations are performed through interpolation between key frames [KSK00]. Zou *et al.* [ZLW03] work with pure geometric relationships between the muscle profile curves and cross sections achieving real time simulations, but their results lack of realism. More recently Kim *et al.* use affine bones to guide the surface deformation of the muscles [KFY10]. They use GPUs and they obtain very fast computation, but their results are not very realistic.

Other works represent muscles using anatomical models. Inaba *et al.* [IMH02] use a three-layer model: bones, muscles and fat tissue. The deformations are produced by a mass-spring system applied over the mass nodes of the muscular layer. Although the movement is generated by a muscular force, the way they get those values is unknown. Also Nedel and Thalmann [NT98] use a three-layer model [ST95] but the shape of the muscles is represented by an implicit surface and the joint motion is set by user intervention. In both cases results are not realistic, but simulations can be done in real time.

Dong *et al.* [DCKY02], as well, propose an anatomically-based approach to model human muscles. The movement of joints and bones produces the deformation, achieved by replacement of the muscle insertions and by re-computation of the muscle shape. Through adding textures and colors got from anatomical images, they achieve realistic results. More recently, Oberhofer *et al.* [OMSA09] use the Host Mesh Fitting technique for predicting muscle deformation during walking and Maurice *et al.* [MSP<sup>+</sup>09] estimate internal deformation combining FEM and subject-specific data. In all these works, like in [DCKY02], movement is achieved by motion capture and visual results are good but computation is very time consuming.

Several works focus on biomechanical accuracy of muscle deformation, consid-

ering the internal arrangement of the fibers, the architecture and the activation of the muscles. In most of them the geometric models are accurate and the visualization is realistic, but unfortunately all these works are far from achieving real time. In this field, Ng-Thow-Hing and Fiume [NF02] model muscles as B-spline solids from contour curves, digitized fibre sets and profile curves and the manipulation of the muscles must be done interactively by the user. Teran *et al.* [TBNF03] also use B-spline solids to represent the fiber directions of the muscles and the geometry is obtained from segmented data [TSB<sup>+</sup>05]. The muscle activation is computed from key-frame poses and the simulation of muscle contractions is done using the Finite Volume Method. Lemos *et al.* present a non-linear FEM to design and simulate a general, variable muscle fibre architecture [LEHW01] [LEHW02]. But no information about calculus time is presented. Later, the same authors applied their FEM method to deform a human muscle using activation relations based on physiologically parameters [LEH<sup>+</sup>03] [LRB<sup>+</sup>05]. The motion is achieved by changing the tendon positions. The method seems to be very accurate, and although only one muscle is represented, it is computationally very expensive.

For analyzing clinical and more complex biomechanical aspects Fernandez and Hunter [FH05] represent the muscles with an anatomically based geometry including information about the fibre directions estimated from anatomy images. The models are customized to patient images using Host Mesh Fitting. Later, Fernandez and Pandy follow a similar approach to carry out experimental validation of subject-specific model simulations [FP06]. Both works present accurate results, but far from real time, and, in them, movement is obtained via patient-specific motion capture.

In the light of the works already presented, it can be noticed that some of them include accurate models of muscles for realistic visualization or biomechanical applications but they don't allow real time. Moreover, most of them simulate the muscle deformation from a specific movement, usually from captured data, key-frame or user interaction. None of them allows the animation in real time of the muscle deformation considering a continuous movement, as locomotion.

In order to have a good approximation of the deformations produced by the movement in each instant of time, we develop a system based on a *Finite Element Method (FEM)*, fed by a force pattern obtained from a *line of action* model, inserted in a skeletal model. The orientation and displacement of the segments of the skeleton come from a hybrid dynamics-kinematics locomotion system. Moreover, our system takes into account anthropometrical characteristics so that different simulations can be generated varying the weight, height or physical constitution of individuals.

### 3 System Overview

Our system, called MOBIL (Muscle defOrmation in Biped Locomotion), is an experimental framework that allows to animate coordinately, both, the global body movement and the local volumetric deformation of the muscles during locomotion. In order to create the external muscle deformation, as in most of the works in computer graphics, the kinematic skeleton drives the motion and the deformation of the muscles attached to it. In our case, the realistic movement of the skeleton is obtained from a dynamic model which is the basis of a subsequent kinematical calculus, and that allows the real time simulation of the locomotion. The system gives the values of the forces that act over the different muscular groups through the muscle action lines, so that the deformation of muscles can be simulated by the FEM system.

Basically, our system is divided in two main phases (see Figure 1): the **skeletal** phase allows to obtain the segment and joint motion (global motion) and the **musculoskeletal** phase that produces the local deformation of the muscles (local motion). As it can be observed, within each phase, the system works with several physically-based models with different level of complexity: *dynamic* and *kinematic* models in the skeletal phase and *muscle line of action* and *finite element* models in the musculoskeletal phase (in each phase, the first model produces the patterns required to “start and control” the second model).

The human body is represented by a musculoskeletal model composed by two layers: a skeletal layer and a muscular layer. The human skeletal model consists of a hierarchical structure of 48 rigid articulated segments (see Figure 2), built in a parametric way from anthropometrical data [Win79] [Pie95]. By changing the values of height and weight a new human skeleton can be generated by the application. In the muscular model, muscles are represented by a volumetric mesh which size and volume are obtained parametrically from the height, weight, biotype and physical constitution.

### 4 Skeletal Phase: Global Motion Simulation

The system developed for the simulation of human motion is based on a “hybrid: dynamic-kinematic” technique [RBS02], that divides each step in two phases, one for the support leg and other for the swing leg. The control scheme followed for the simulation of each locomotion step is presented in Figure 3. Acceleration changes in walking can be simulated in our system since step symmetry is not assumed [BTT90].

The anthropometric differences between individuals and the differences in motions can be easily reproduced by high level parameters. In this way, different animations can be achieved varying step speed, step frequency or step length and the weight, height and physical constitution of the person. Even more, there are

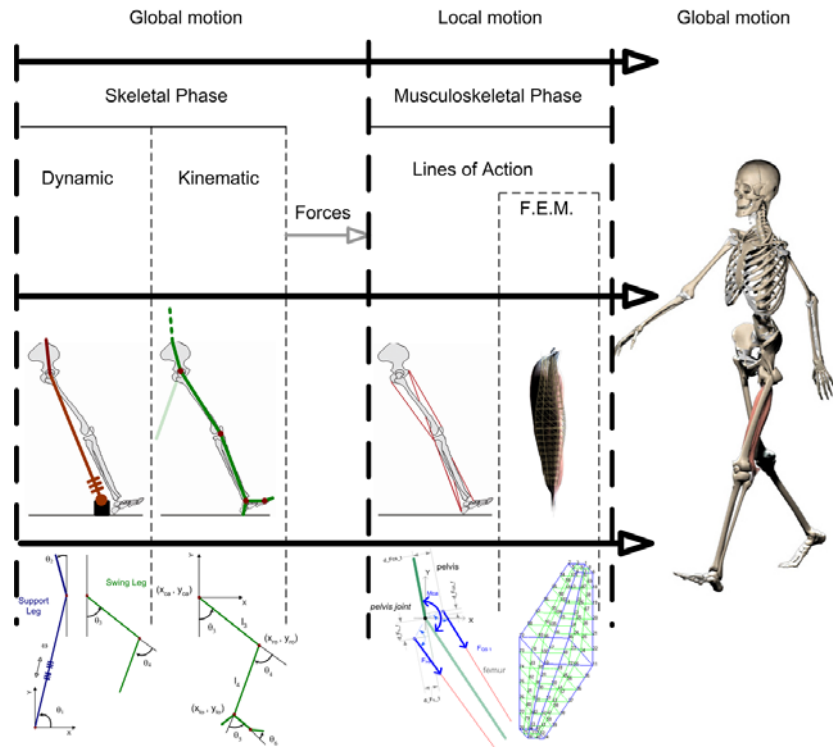


Figure 1: The different models applied in our system are shown from left to right. The calculus of global motion in the skeletal phase is achieved through a dynamic and a kinematic model that allow to obtain the required forces. With these data, the musculoskeletal phase produces the local deformation of the muscles during locomotion using a line of action model and a FE Model.

30 differentiation parameters in the system (such as limits and angular values of pelvic swinging, pelvic rotation, shoulders, ankles, insteps, elbows, etc) that allow the characterization of each animation individually [Bal04].

#### 4.1 Dynamics-based model

The basic pattern of motion is obtained from the high level parameters using *direct dynamics*. The Lagrange-Euler method is used to deduce the motion equations from a simplified model [Win90]. The energy of the system allows the identification of the interaction and coupling forces presented according to each generalized coordinate  $q$ :

$$\vec{F}_q = \frac{d}{dt} \left( \frac{\partial T_q}{\partial \dot{q}} \right) - \frac{\partial T_q}{\partial q} + \frac{\partial U_q}{\partial q} \quad (1)$$

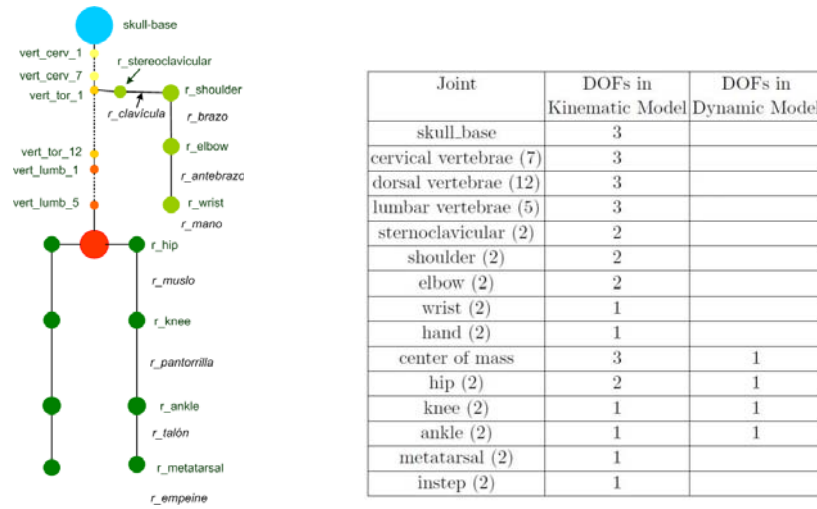


Figure 2: Hierarchical structure of the skeleton (left). Degrees of Freedom (DOFs) of each joint (right).

where  $T_q$  is the kinematic energy,  $U_q$  the potential energy,  $q$  the generalized coordinates and  $\vec{F}_q$  the generalized forces.

The method produces a multivariable system of second-order differential equations, nonlinear and strongly coupled, whose expression is  $[A]\ddot{\vec{q}} = B(\vec{q}, \dot{\vec{q}})$ , with the generalized coordinate vector  $\vec{q}$  is:  $\vec{q} = [\omega, \theta_1, \theta_2]^T$  for the support leg and  $\vec{q} = [\theta_3, \theta_4]^T$  for the swing leg. The deduction of the final expressions for each generalized coordinate can be found in [RBS02].

The reference's system for the dynamic model of both legs can be observed in Figure 4.

In the support leg, the longitudinal generalized force  $F_\omega$  simulates the flexion and extension of the knee and the ankle, supplying the characteristic sinusoidal movement of the mass centre. The torque  $F_{\theta_2}$  keeps the upper body upright and gives the up and down smooth hip movement. While the torque  $F_{\theta_1}$  represents the muscular actions that, during 20% of the locomotion cycle, produce the rotation of the support leg that makes the body moves forward [BC89]. In the swing leg, instead, the torque  $F_{\theta_3}$  corresponds to the interaction between the hip and the thigh, while  $F_{\theta_4}$  represents the actions produced in the knee by the muscles of the thigh and the calf.

The resolution of the complex motion equations of the proposed dynamic model are simplified subdividing the support and swing states in subphases, as it is detailed in Figure 5.

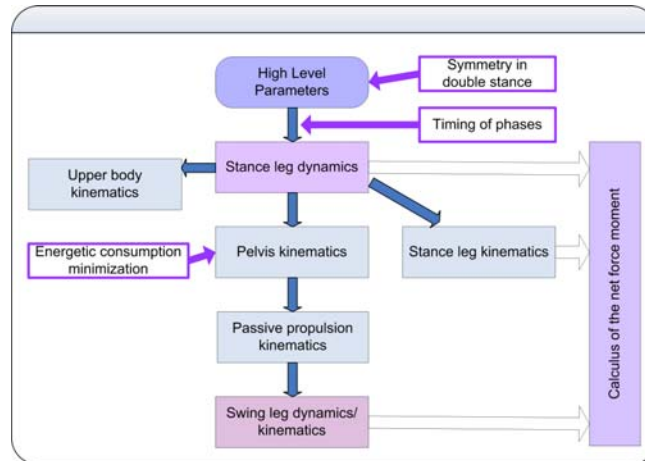


**Figure 3:** Description of the global motion system

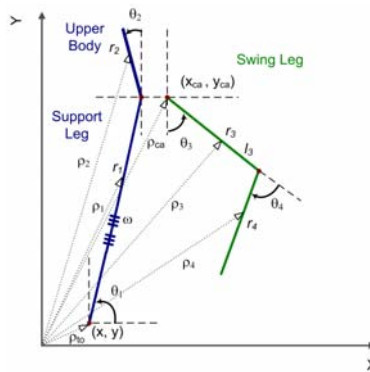


**Figure 4:** Dynamic model of the support and the swing leg

The value of each generalized force depends on the subphase and is calculated recursively, verifying if it fulfills some boundary conditions. These conditions are set from the empirical knowledge of human locomotion: timing of phases, double support symmetry and energetic minimization [BC89].

The numerical resolution method implemented is a multi-step  $n$ -dimensional predictor-corrector algorithm with adaptative control of the integration step [BF85]. An Adams-Bashforth algorithm is used as predictor while a Moulton-Adams algorithm is used as corrector. The system is initialized with a 4<sup>th</sup> order Runge-Kutta method.

### 4.2 Kinematics-based model

*Kinematics* constraints are applied to the movement of all those segments and angles of the articulated model that are not direct result of the dynamic simulation, up to the 48 segments that constitute the hierarchical structure of the skeleton. For this purpose a new timing of phases is considered (see Figure 5).

The kinematics of the support leg reflects the biomechanical performance of the knee and the ankle. They absorb the collision of the heel, soften the transition between the swing and support states and keep the major possible height of the mass center.

The most important movements of the pelvis in real locomotion, considered in our system are (see Figure 6):

- pelvic rotation: increases the step length (produced in the transverse plane),
- pelvic swinging: produces one hip to be higher than the other (produced in the coronal plane),
- lateral displacement: transfers part of the body weight to the support leg (also in the coronal plane).

The kinematics of the swing leg completes the foot movement by linear interpolation between the different subphases.

The upper body kinematic model simulates all the vertebral column gathering the movements according to lumbar, thoracic and cervical vertebrae. Each vertebra only makes rotation movements with respect to the previous one. The pelvic rotation and the rotation of the shoulders in the opposite direction are compensated along the vertebral column in such a way that the head always remains in the walking plane. In the transverse plane, the shoulders rotate in an opposite direction and proportionally to the pelvis. In the walking plane, instead, the arms rotate proportionally to the “dynamic” angle of the hip of the opposite leg and the forearms are directly interpolated between the experimental values.



Figure 5: Timing of phases of the support and swing legs

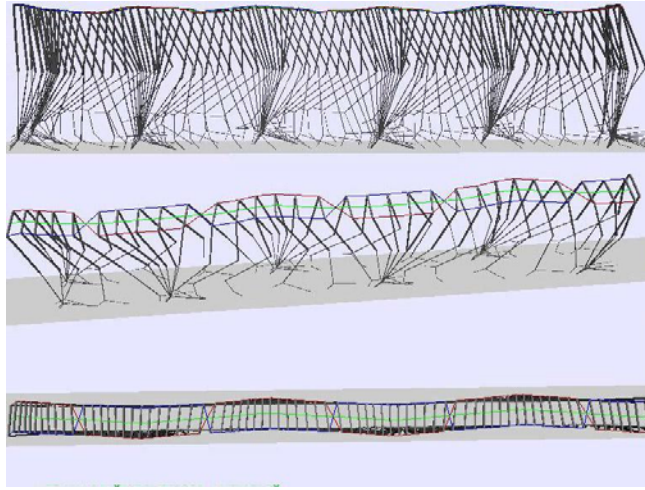


**Figure 6:** Pelvis movement during locomotion

### 4.3 Analysis of the motion

Although models with different level of complexity are used: very simple for dynamics and more complex for kinematics (see Figure 2, Section 3), the movement remains continuous applying theorems of energy conservation between phases (support and swing phase) and between two consecutive steps.

The implemented method allows the real time simulation of global motion of the skeleton of persons with different anthropometrical characteristics. The final visualization can be represented as a stick model, a wireframe model or an anatomical surface model. Table 1 shows the CPU times resulting from the computation of various locomotion sequences varying the number of steps and using a Pentium IV computer at 2800 MHz. All the simulations correspond to a person of 80 kg of weight and 1.80 m of height, walking at *natural step* (5 km/h).

**Table 1:** Calculus time with a Pentium IV at 2800 MHz

Locomotion Steps	Simulated Time	Frames	CPU Time
3	1.27 sec	30	0.078 sec
4	1.84 sec	44	0.144 sec
5	2.4 sec	58	0.174 sec
10	5.2 sec	128	0.312 sec
20	10.76 sec	267	0.612 sec

Variations of the anthropometric data like individuals with different height or weight change the values of the parameters considered in the dynamic and kinematic equations and, therefore, the final locomotion is also modified. As an example, Figure 7 shows the changes produced in the trajectory of the center of mass of the body by means of the gravity influence for individuals with different weights (65 Kg, 80 Kg and 120 Kg), walking at the same speed (5 km/h). Also, it must be taken into account that during normal locomotion, the center of mass moves up and down, rhythmically. The upper point occurs when the support leg is in its midstance, and the lower point occurs in the double support phase. Therefore, if the step length increases, the trajectory of center of mass varies, making the lower point to descend even more.

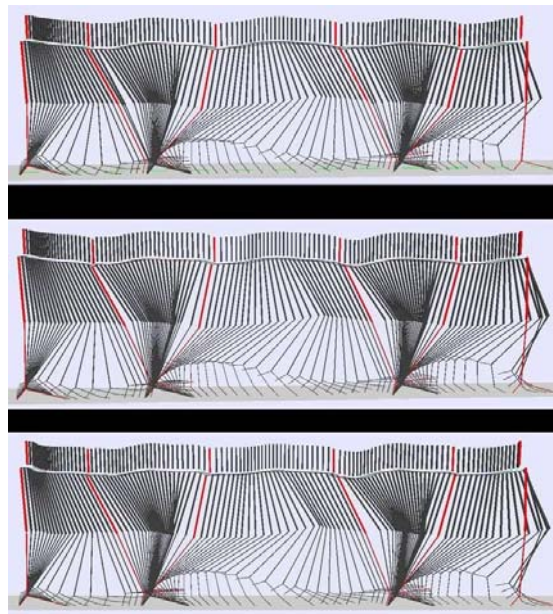


Figure 7: Changes of the anthropometric data: individuals with 65 Kg, 80 Kg and 120 Kg of weight (from top to bottom) walking at the same speed (5 km/h).

The data values obtained from our locomotion system have been compared and verified with experimental data from biomechanical studies. Figures 8, 9 and 10 reflect the comparisons of our data with the temporal patterns of the joint angles [Win87] of the hip, knee and ankle, respectively. There is a clear similarity between the superior and inferior limits, the growth intervals and the slopes. The values of the simulated movement are, therefore, very close to real human walking.

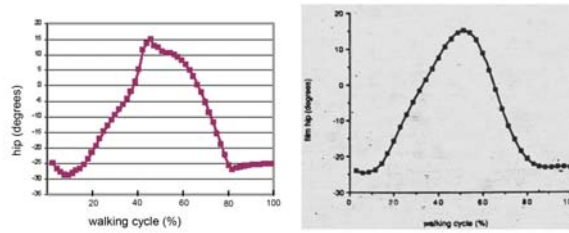


Figure 8: Comparison of the hip angular values obtained from our simulation (left) and from experimental data (right)

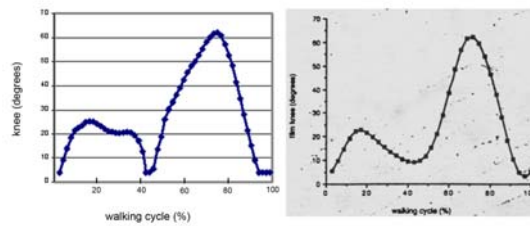


Figure 9: Comparison of the knee angular values obtained from our simulation (left) and from experimental data (right)

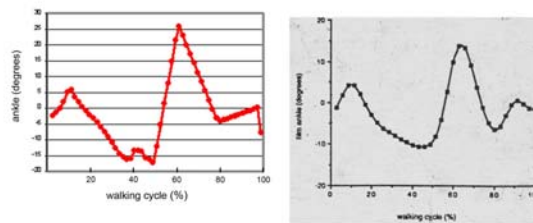


Figure 10: Comparison of the ankle angular values obtained from our simulation (left) and from experimental data (right)

The correct behavior of the system dynamics has been also verified comparing the ground reaction force obtained with Whittle’s experimental data [Whi03] (see Figure 11).

Although these patterns use to present a wide range of values depending on the gender, locomotion parameters and anthropometrical characteristics, it can

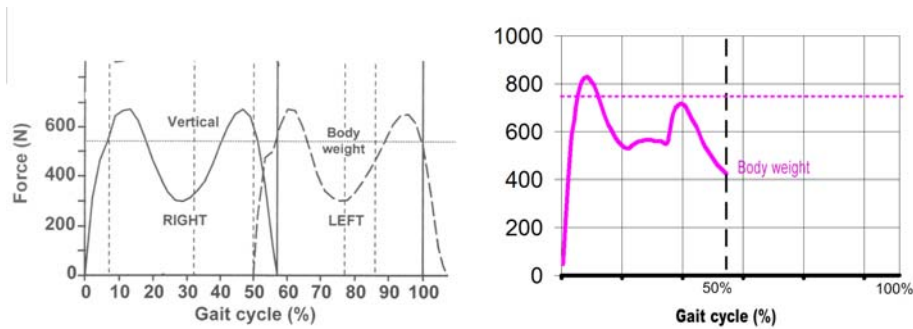


Figure 11: Comparison of the ground reaction force of our simulation (left) with experimental data (right)

be observed in the figures the same order of magnitude and a clear similarity in the growth and slopes intervals. In this way, the behavior of our system is very close to real data.

The dynamics and kinematics of the system also allows to get the values of moments and forces that act over the different muscular groups by means of the well-known “Free Body Diagrams”. This information is used for computing the deformation of the muscles in the musculoskeletal phase.

## 5 Musculoskeletal Phase: Local Deformation

In order to obtain a system which comprises both global movement and local deformations, we take into account muscular activity in the previous developed skeletal phase, emerging the musculoskeletal phase of the system.

The pattern of the forces that acts over the muscles is obtained from a *line of action* model inserted in the skeletal model. Since individual human muscle forces are not trivial to estimate using the current available measurement techniques, the line of action model is used to estimate the force of a specific group of muscles. These force values constitute the low level entry and they suitably condition the finite element model (FEM) that calculates the volumetric deformation of the lower limb muscles during the global locomotion movement.

In this phase the muscles with similar action during locomotion are gathered in groups, like in many other research works [Pau67] [ZNK02] [Whi03]. Considering their influence in the external shape of the leg during locomotion, the muscular groups (and the corresponding muscles) taken into account in this work are:

- Quadriceps (QS): rectus femoris, vastus medialis, intermedius and lateralis.

- Hamstrings (HM): biceps femoris, semitendinosus and semimembranosus.
- Tricep Surae (TS): gastrocnemius, soleus and plantaris.

In order to represent persons with different anthropometrical characteristics, the values of height, mass, biotype and physical constitution are considered to customize the geometric data of the muscles. The muscular properties used in this work are taken from [Pie95] and correspond to muscle length, tendon length, muscle belly length and mass. All the muscles are assumed to be parallel fibered.

The integration of the volumetric model into the skeletal phase is done by means of the muscle line of action. In this way, the muscular deformation behavior is similar to the real deformation and it is coordinated with the motion of the legs.

The different anthropometrical characteristics that can be established in the skeletal phase (height, weight, step length, step speed, step frequency) allow to obtain different locomotions, and, in consequence, different values of forces are produced by the line of action model. This, in addition to the fact that the size and length of a muscle depends on the height and weight of the person, make it possible to simulate the deformation of an specific muscle with variations regarding the individual anthropometric characteristics.

### 5.1 Muscle Action Line Model

The action line model is used in two moments of the work sequence: before the FEM calculus, to estimate the force values of a specific group of muscles; and after the FEM calculus, to verify the results of the deformation in the global locomotion movement.

The lines of action approximate the position and the orientation of each muscular group according to the body movement. The endpoints of the line are calculated in the centroid of the origin and insertion points of each muscle (see Figure 12). Most lines of action are represented by straight lines joining origin to insertion [DL95], except in the quadriceps case, in which a *special* line of action simulates the kneecap tendon and the set is comprised by the kneecap and the ligaments [Pie95]. In order to simplify, the action line model uses the reduction method to distribute the forces in the articulations, gathering the muscles that develop the same action [AKC95].

As the macroscopic behavior of each muscle is known and it is coordinated with the different frequencies of the locomotion gait, it is possible to define the muscle material with a linear behavior “similar” to the no linearity of the muscle tissue and with suitable propagation velocities. Once the material is determined, a linear elastic approximation is introduced in the line of action model.

The force is simulated by a *muscular tissue spring*, with similar section to the surface of impose of the tensor stress, in the mesh that represents the muscle in

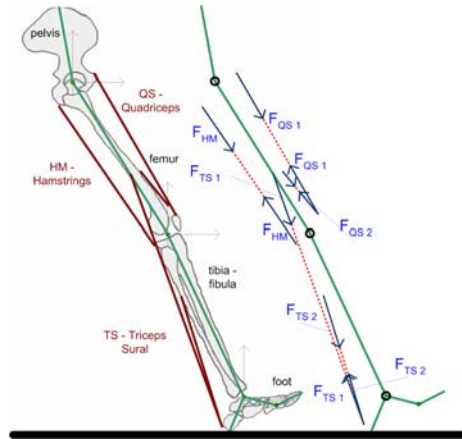


Figure 12: Action lines of the following muscular groups of the lower limbs: HM-Hamstrings, QS-Quadriceps and TS-Triceps Sural (left). Representation of the forces that act over each muscular group (right).

the FEM calculus. The following spring expression determines the muscle force:

$$F_m = -k(L_m - L_o) \quad (2)$$

where  $F_m$  is the muscle force,  $L_m$  is the muscle spring length at any moment,  $L_o$  is length of the spring in rest and  $k$  is the stiffness constant.

So that, the force pattern that acts over each muscular group,  $F_m$ , can be achieved introducing in Equation 2 the  $L_m$  values got from the line of action model and the stiffness constant  $k$ . The value of this constant  $k$  is calculated from the Young's modulus used to define each muscular group material in the FEM model, and it is deduced as:

$$k = E s/L_o \quad (3)$$

where  $s$  is the muscle spring section and  $E$  is the Young's modulus, that, in this case is obtained considering the Hooke law that sets  $\sigma = E\epsilon$ , where  $\sigma$  is the stress and  $\epsilon$  the strain [Sok56], and taking into account that  $\sigma = F_m/s$  and  $\epsilon = (L_m - L_o)/L_o$ .

It's important to point out that this approach obeys to the necessity of introducing in the FEM model not only the muscle forces but the "forces that act over the muscle" (that not participate in the motor activity but cooperate in the muscle motion and elongation). The use of the lines of action allows to approximate the force of each muscle from the result that produces over all the locomotion cycle, so that the problem phenomenology remains.

### 5.2 Muscle Deformation

Muscles have a non-linear, viscoelastic stress-strain relationship [Fun93], and this is the approach usually used in biomechanical problems where the accuracy prevails over the computational cost. As real time simulation requires certain conditions of speed, robustness and satisfactory visual result, we model the deformation using a Finite Element approximation of linear elasticity.

The idea of the Finite Element Method is that an object can be seen as a continuum, that can be approximated in the space by dividing it into a mesh of discrete elements. The muscle is modeled as a three-dimensional linear elastic solid that satisfies the governing Lagrange equations of motion [Sok56]:

$$M\ddot{\mathbf{d}} + C\dot{\mathbf{d}} + K\mathbf{d} = \mathbf{f} \tag{4}$$

where  $M$  is the mass matrix,  $C$  is the damping matrix and  $K$  is the stiffness matrix. The coefficients of these matrices are related with the material properties of the muscle:  $M$  is obtained from the muscular density,  $C$  from the absorption of the forces while  $K$  is obtained from the elastic properties known as *Young's modulus* and *Poisson's coefficient*.  $\mathbf{f}$  is the load vector, whose coefficients are taken from the external forces applied to the system (time independent forces) and from the line of action model (time dependent forces). Finally, vector  $\mathbf{d}$  is the unknown variable of the system that corresponds to the displacement of the unconstrained mesh nodes while  $\dot{\mathbf{d}}$  is the velocity and  $\ddot{\mathbf{d}}$  the acceleration.

In order to calculate the response of the muscle, the governing differential equations (given by Equation 4) have to be solved subject to the boundary conditions, that, in this case, are given by the vertices of the mesh which belong to the origin of the muscle.

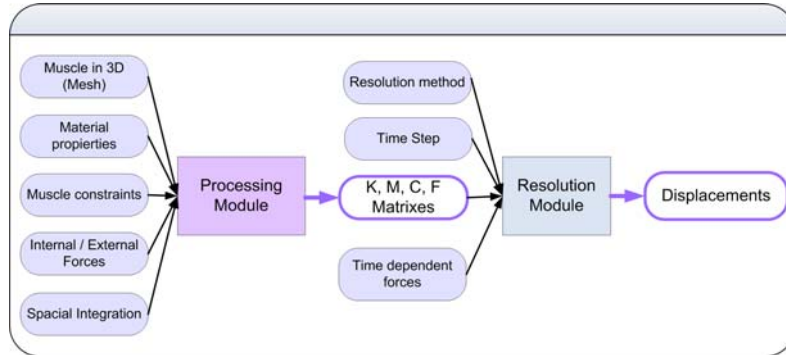


**Figure 13:** Description of the developed FEM system

The general description of our FEM software is shown in Figure 13. The

system is split in two main blocks. In the first block the entry data are processed in order to get the vectors and matrixes that make up the equation system. The second block obtains the solution of the system, that can be either static or dynamic. The static system ignores the velocity and acceleration terms, so the system equation can be written as  $K\mathbf{d} = \mathbf{f}$ . Solving the linear sparse system, the displacements for the nodes of the mesh are obtained [Ueb97].

However, to determine the evolution of an object deformation through time, a discretization of the time-dependent variables in Equation 4 must be done, leading to:

$$M\ddot{\mathbf{d}}(t) + C\dot{\mathbf{d}}(t) + K\mathbf{d}(t) = \mathbf{f}(t) \quad (5)$$

In our system, the calculus of the displacement, velocity and acceleration at each step time can be obtained by the resolution techniques corresponding to the Newmark methods [SSK89].

## 6 Experimental Results

The MOBiL system allows to present different graphical results of the movement in humans with different anthropometric characteristics, such as: *real time* visualization of the human body as a skeleton, wireframe model or anatomical surface model; VRML file with the information about the geometry and the movements of the body; files with the GL coordinates (one for each time step) [NDW93]; still images, 3D stereoscopic images [Ste97] or video sequences.

Different experimental results obtained with our system are shown in this section. First, we describe the simulation of the muscle deformation, second, we present the coordinated animation of the muscle deformation during locomotion, and finally, the calculus time is shown.

### 6.1 Simulation of muscle deformation

The MOBiL system allows to generate the simulation of the muscle deformation produced during human locomotion. The muscle elastic properties considered in this work are: *density* = 1000 kg/m<sup>3</sup>, *Young's Modulus* = 1.06667e+4 Pa and *Poisson's coefficient* = 0.3333. The *Young's Modulus* is similar to the one used in [ZM99] and the *Poisson's coefficient* was found to be a good compromise between the requirement of the constitutive modeling and the computational cost of the FEM [MSG08]. The size of the muscular group mesh is got from the implemented parametrization algorithm, considering, in this case, a man of 1.80 m of height and 80 kg of weight. The muscle is modeled as a mesh constituted by 8-node 3D brick elements, since hexahedric elements preserve better the strain propagation [MMP99].

The performed simulation is carried out with 320 trilinear hexahedric elements and 525 nodes, and with  $\Delta t = 0.001$  as integration step. In order to get the displacements of the nodes in the FEM system the Newmark Central Average Acceleration method is used.

Figure 14 presents three snapshots of the deformation of the hamstring muscular group rendered with a wireframe model.

The dynamic model shows the changes in a muscle when the force is applied at the bottom, while it is fixed at the highest points. The input forces come from the line of action model and are represented below the “Input” label, at the left side of the figure. In the right side, below the “Output” label it is shown the displacement produced in the mesh nodes by the FEM calculus. Both graphs represent the data corresponding to one node of the mesh. In the central part of the figure, the deformed mesh is presented at different time moments. These results remain similar with other integration methods.

The experimental results obtained from the biomechanical literature [ABD01] [VHBH90] [DASM96] verify the displacement values achieved with our MOBiL system. Figure 15 presents a comparison between the length changes of the “hamstring muscular group” obtained in our system and those published by Delp *et al* [DASM96]. In order to make the comparison our data have been scaled and turned to Delp’s metric.

## 6.2 Muscle deformation during locomotion

The system allows to generate the animation of the human motion with the muscle deformation for each instant of time, in real time and in a coordinated way. So that, it is possible to observe the changes produced in the shape of the lower limb muscles while a person walks. A snapshot of a simulation can be seen in Figure 16 (left) in which the body is represented as a skeleton and the muscle is represented with a realistic surface 3D model extracted from medical images. A whole locomotion sequence can be observed in Figure 16 (right).

The FEM mesh nodes are used as control points of the anatomical surface model of the hamstring muscle in order to improve the visual aspect of the muscle’s deformation without increasing the calculus time (see Figure 17).

## 6.3 Calculus Time

The calculus of the skeletal phase clearly allows to obtain real time simulations (see Table 1). However, and in order to determine the possibility of doing the simulation in real time of several muscle deformations at the same time, we did several tests varying the values of different parameters (like spatial resolution, time integration step and CPU) and considering the following Newmark resolution methods: Explicit Central Difference (ECD), Implicit Central Difference (ICD) and Constant Average Acceleration (CAA).

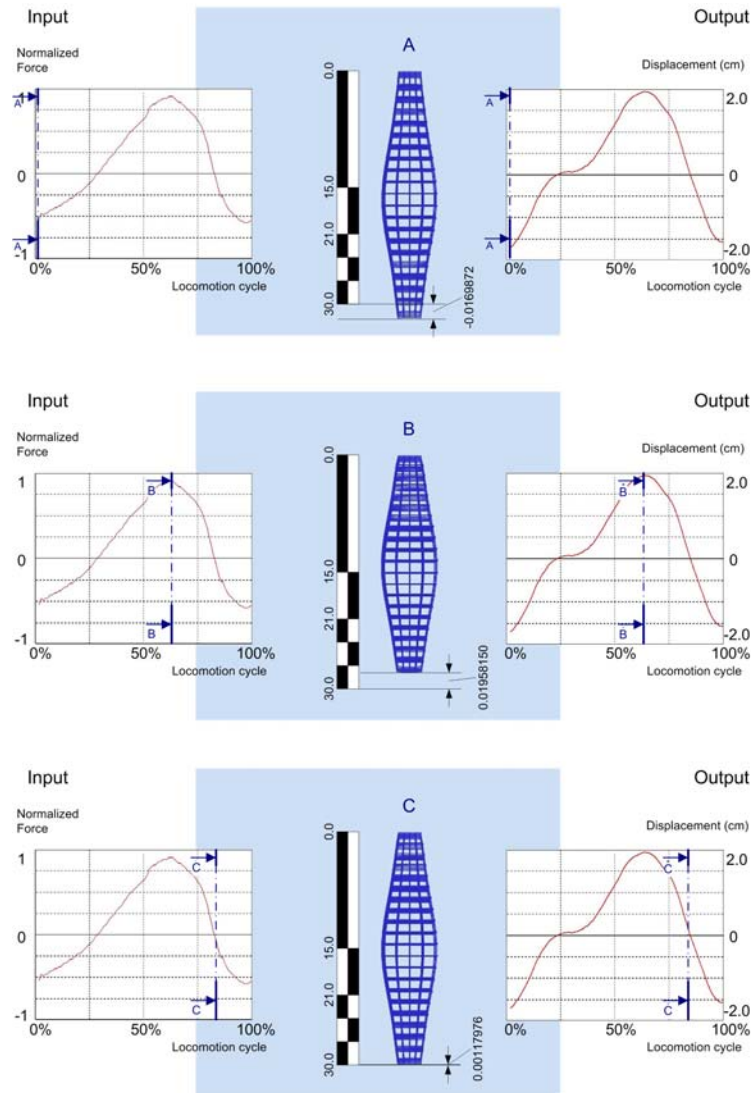


Figure 14: Hamstring deformation at different time moments of the locomotion cycle: “A” (top), “B” (middle) and “C” (bottom). The “Input” label represents the forces that come from the line of action model (left) while the “Output” label shows the displacement produced in the mesh nodes by the FEM calculus (right). The resulting hamstring mesh for each moment is shown in the central part of the figure.

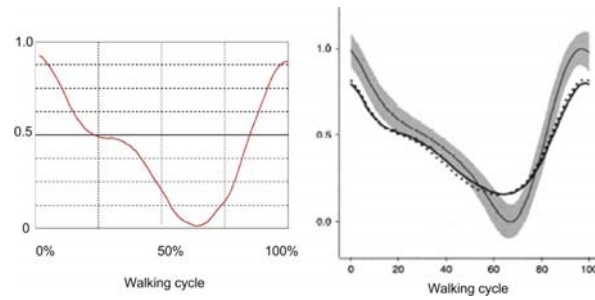


Figure 15: Comparison of the hamstring length. At left, the results obtained with MOBIL. At right, the results of [DASM96], in which the grey area corresponds with normal locomotion.

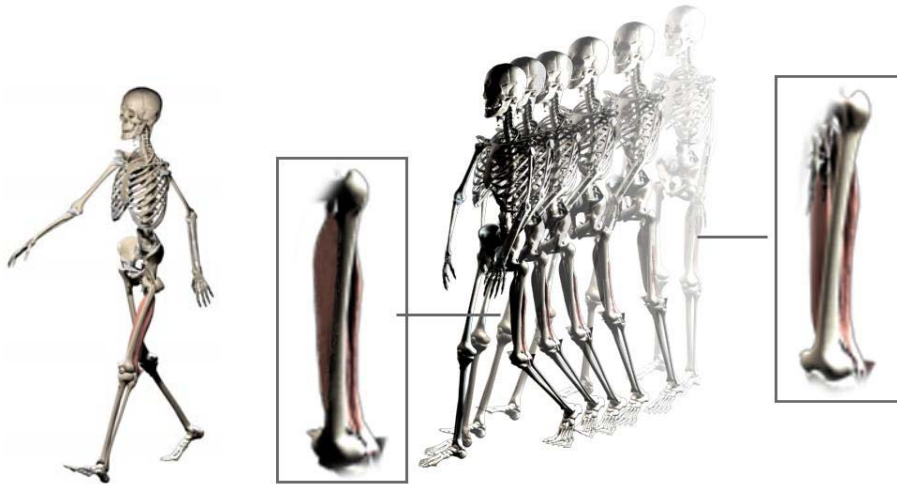


Figure 16: Snapshot of a human skeleton with the hamstring muscular group, both represented by an anatomical surface model (left). Deformation of the hamstring muscular group during a locomotion sequence (right)

The comparison of the calculus time for 1 second of simulation, in a Pentium IV at 2800 MHz, for the three resolution methods, is shown in Figure 18. In Figure 18 (left) a mesh of 525 nodes (minor  $\Delta x = 0.0075$ ) is used while in Figure 18 (right) the mesh has 81 nodes (minor  $\Delta x = 0.015$ ). The size of  $\Delta x$  determines the larger value of  $\Delta t$ , so that  $\Delta t = 0.004$  can't be used for a mesh of 525. For details of the features of each method regarding the number of nodes  $\Delta x$  and the integration step  $\Delta t$ , see [BW76] [DT81] [GHR87].

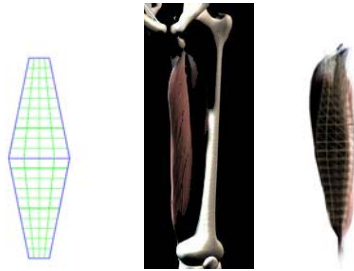


Figure 17: Hamstring muscular group represented with a mesh of 525 nodes (left) and with an anatomical surface model (center). The superposition of both (right) shows the anatomical surface that is modified by the FEM mesh nodes used as control points

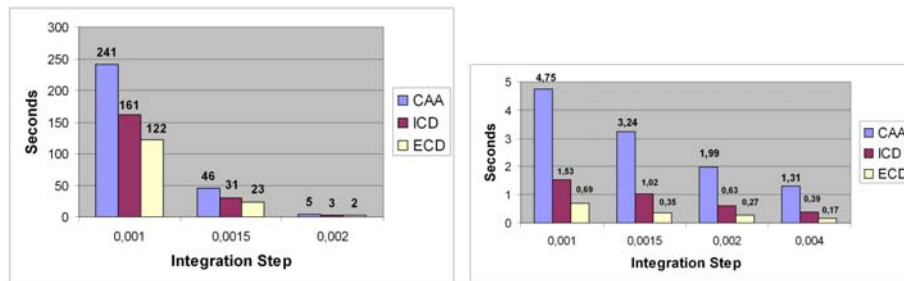


Figure 18: Comparison of the computation time varying the integration step using different resolution methods for a mesh with 525 nodes (left) and with 81 nodes (right), for 1 second of simulation

Although the result of using the CAA method with 525 nodes is more accurate, a comparison with the ECD method with 81 nodes reflects that qualitatively both methods show a satisfying agreement (see Figure 19). Therefore we considered the ECD method as the most suitable since it allows to change precision for more muscles, in a simulation in real time.

Therefore, considering the results of the three methods, the ECD method was selected because it is faster and offers a good relationship between computation time and accuracy. The ICD method is a little slower than ECD, but the principal problem is that it requires a minor critical time step  $\Delta t_{cr}$ . On the other hand, the CAA method is not limited by a critical time step  $\Delta t_{cr}$ , so a larger  $\Delta t$  could be used without losing stability but, unfortunately, it is very slow.

In all the cases, the maximum size of each finite element, and so, the number of nodes of the mesh, is determined from the fundamental length wave [Mas03].

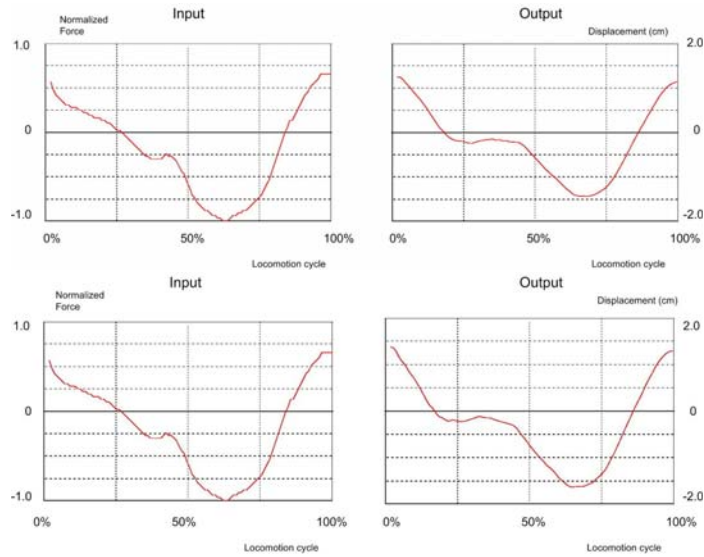


Figure 19: Comparison of the results of the simulation using the CAA method with 525 nodes (above) and the DCE method with 81 nodes (below).

In our case, a final value of  $\Delta x \leq 0.030m$  is obtained. However we decided to use a mesh with more level of detail, getting  $\Delta x = 0.015m$ , in order to get more accuracy and because with this value the method is fast enough.

The Explicit Central Difference method requires the time step to be inferior to the critical integration step  $\Delta t \leq \Delta t_{cr}$  that in this case is  $\Delta t_{cr} = 0.0037$  with  $\Delta x = 0.015$  (81 nodes) [BW76].

The variation in the number of nodes of the mesh considerably affects the time employed for the simulation of the muscle deformation. The comparison of the calculus time between the different size of elements  $\Delta x$ , and so the number of nodes, for 1 second of simulation, is shown in Figure 20 (left). The computation was done with the ECD method and  $\Delta t = 0.001$  as integration step because the use of a minor  $\Delta x$  implies  $\Delta t_{cr}$  must also be minor. Figure 20 (right) reflects the time variation, in seconds, of considering different values of integration step for the selected  $\Delta x$  (81 nodes) and the ECD resolution method in a Pentium IV at 2800 MHz for 1 second of simulation. As an agreement between speed and accuracy, the final value of  $\Delta t = 0.002$  was considered. However, for the calculus of more than one muscular group in real time, the value of  $\Delta t$  could be increased.

From these time calculations, it can be deduced that the three more important muscular groups of the lower limbs can be simulated in real time. Also a

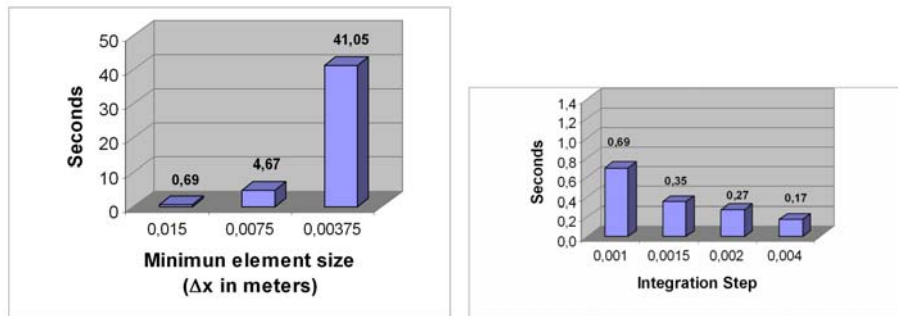


Figure 20: Comparison of the computation of the ECD method using meshes with different number of nodes (left): 81 ( $\Delta x = 0.015$ ), 525 ( $\Delta x = 0.0075$ ) and 3321 ( $\Delta x = 0.00375$ ), and considering different integration steps (right), for 1 second of simulation

four muscular group (tibialis anterior) could be calculated with enough accuracy if the integration step is increased to  $\Delta t = 0.003$ .

## 7 Conclusions and Future Work

This paper describes a system for real time simulation of a skeletal global motion coordinated with the local deformation of the muscles, for individuals with different anthropometrical characteristics. Unlike most previous works, different animations can be achieved in real time varying high level parameters as step speed, step frequency or step length and the weight, height, biotype and physical constitution of the person. No human interaction or captured data are needed.

For this purpose, our system works with different complexity models, going from global to local and from the skeleton to the muscles, passing through a line of action model that considers the moments and forces that act over the muscles, the muscle geometry and the muscle material properties. The animation of the muscles' deformation of a person during locomotion can be visualized in real time solving the FEM system with an Explicit Central Difference method (ECD) and using a suitable size for the elements of the muscular mesh. With the proposed method, the three more important muscular groups of the lower limbs (hamstrings, quadriceps and triceps surae) can be animated in real time. However, in order to work with meshes with more level of detail or to include more muscular groups is essential to include parallelism techniques. For this purpose, we will work with a Beowulf cluster [SGMB03], using the standard MPI library [WSG<sup>+</sup>98] for the communication between the different processes.

All the data values obtained from our system have been validated with experimental data published in biomechanical studies, however, we could improve the realism taking advantage of volume information in FEM, considering the internal composition of muscles (fibers, angle of pennation) [NF02] [LRB<sup>+</sup>05] [TSB<sup>+</sup>05] or taking into account the anisotropic behavior of the muscle [BR08]. Other possibility to improve realism in the visualization could be the addition of a skin layer in our model, like in [WV97], [SPCM97] or [YG06].

For the moment good visual results in the appearance of the muscle deformation are achieved by using a realistic and accurate surface model extracted from anatomical data controlled by the nodes of the FEM mesh. The results obtained with our system allows to increase naturalness and realism to virtual actors in environments or computer games in which real time constraints make impossible to obtain a precise and exceptional visual quality.

### Acknowledgements

This work was partially supported by the University of Zaragoza through the “AVIM- Agentes Virtuales Inteligentes y Multimodales” Project.

The authors want to thank the collaboration of Jorge López in this work.

### References

- [ABD01] Arnold, A., Blemker, S., and Delp, S.: Evaluation of a deformable musculoskeletal model: application to planning muscle-tendon surgeries for crouch gait; *Annals of Biomedical Engineering*, 29:263–274, 2001.
- [AKC95] An, K., Kaufman, K. R., and Chao, E.: *Three-Dimensional Analysis of Human Movement*, chapter Chapter 10: Estimation of Muscle and Joint Forces, pages 201–214 Human Kinetics, 1995.
- [Bal04] Baldassarri, S.: *Simulación Eficiente de Fenómenos Físicos en Medios Continuos: Su Aplicación a la Locomoción Humana* PhD thesis, Departamento de Informática e Ingeniería de Sistemas, Universidad de Zaragoza, Spain, December 2004.
- [BC89] Bruderlin, A. and Calvert, T. W.: Goal-directed, dynamic animation of human walking; *Computer Graphics*, 23(3):233–242, July 1989.
- [BF85] Burden, R. L. and Faires, J. D.: *Numerical Analysis* Prindle, Weber & Schmidt, 1985.
- [BR08] Bol, M. and Reese, S.: Micromechanical modelling of skeletal muscles based on the finite element method; *Computer Methods in Biomechanics and Biomedical Engineering*, 11(5):489–504, 2008.
- [BTT90] Boulic, R., Thalmann, N. M., and Thalmann, D.: A global human walking model with real-time kinematic personification; *The Visual Computer*, 6(6):344–358, December 1990.
- [BW76] Bathe, K.-J. and Wilson, E.: *Numerical Methods in Finite Element Analysis* Prentice-Hall, 1976.
- [CSC10] Correa, C., Silver, D., and Chen, M.: Constrained illustrative volume deformation; *Computer Graphics*, 34:370–377, 2010.

- [CZ92] Chen, D. T. and Zeltzer, D.: Pump it up: Computer animation of a biomechanically based model of muscle using the finite element method; *Computer Graphics (SIGGRAPH '92 Proceedings)*, 26(2):89–98, July 1992.
- [DASM96] Delp, S. L., Arnold, A. S., Speers, R. A., and Moore, C. A.: Hamstrings and psoas lengths during normal and crouch gait: Implications for muscle-tendon surgery; *Journal of Orthopaedic Research*, 14(1):144–151, 1996.
- [DCKY02] Dong, F., Clapworthy, G. J., Krokos, M. A., and Yao, J.: An anatomy-based approach to human muscle modeling and deformation; *IEEE Transactions on Visualization and Computer Graphics*, 8(2):154–170, 2002.
- [DL95] Delp, S. L. and Loan, J. P.: A graphics-based software system to develop and analyze models of musculoskeletal structures; *Computers in Biology and Medicine*, 25(1):21–34, 1995.
- [DT81] Dhatt, G. and Touzot, G.: *Une Présentation de la Méthode des Éléments Finis* Presses de l'Université Laval, 1981.
- [Duf07] Duffy, V. G., editor *Digital Human Modeling*, volume 4561 of *Lecture Notes in Computer Science* Springer, 2007.
- [FH05] Fernandez, J. W. and Hunter, P. J.: An anatomically based patient-specific finite element model of patella articulation: Toward a diagnostic tool; *Biomech. Model Mechanobiol.*, 4:20–38, 2005.
- [FP06] Fernandez, J. W. and Pandy, M. G.: Integrating modelling and experiments to assess dynamic musculoskeletal function in humans; *Experimental Physiology*, 91:371–382, 2006.
- [Fun93] Fung, Y.: *Biomechanics - Mechanical Properties of Living Tissues* Springer-Verlag, 1993.
- [GHR87] Geradin, M., Hogge, M., and Robert, G.: *Finite Element Handbook*, chapter 1: Solution Methods, Part 4: FEM Computations, pages 4.54–4.103 McGraw-Hill, 1987.
- [IMH02] Inaba, H., Miyazaki, S., and Hasegawa, J.: Muscle-driven motion simulation based on deformable human model constructed from real anatomical slice data; In Perales, F. and Hancock, E., editors, *Articulated Motion and Deformable Objects*, volume 2492 of *Lecture Notes in Computer Science*, pages 32–42. Springer, 2002.
- [KFY10] Kim, B., Feng, W., and Yu, Y.: Real-time data driven deformation with affine bones; *The Visual Computer*, 26:487–495, 2010.
- [KSK00] Komura, T., Shinagawa, Y., and Kunii, T. L.: Creating and retargetting motion by the musculoskeletal human body model; *The Visual Computer*, 16(5):254–270, 2000.
- [LEH<sup>+</sup>03] Lemos, R., Epstein, M., Herzog, W., Kawakami, Y., Kurihara, T., and Wyvill, B.: Modeling the mechanical behavior of skeletal muscle at different structural levels using a continuum approach; Sydney. Australia, August 2003.
- [LEHW01] Lemos, R., Epstein, M., Herzog, W., and Wyvill, B.: Realistic skeletal muscle deformation using finite element analysis; In *Proceedings of the 14th Brazilian Symposium on Computer Graphics and Image Processing*, pages 192–199, October 2001.
- [LEHW02] Lemos, R., Epstein, M., Herzog, W., and Wyvill, B.: Modeling and visualization of the mechanical behaviour of skeletal muscles using a continuum approach; In *Proceedings CD of the IV World Congress Biomechanics. Canada.*, August 2002.
- [LGK<sup>+</sup>09] Lee, D., Glueck, M., Khan, A., Fiume, E., and Jackson, K.: A survey of modeling and simulation of skeletal muscle; Technical report, University of Toronto, 2009.
- [LRB<sup>+</sup>05] Lemos, R., Rokne, J., Baranoski, G., Kawakami, Y., and Kurihara, T.: Modeling and simulating the deformation of human skeletal muscle based

- on anatomy and physiology; *Computer Animation and Virtual Worlds*, 16:319–330, 2005.
- [Mas03] Mascaró, M.: *Modelo de Simulación de Deformaciones de Objetos Basado en la Teoría de la Elasticidad* PhD thesis, Universitat de les Illes Balears, 2003.
- [MG06] Moeslund, T. B. and Granum, E.: A survey of computer vision-based human motion capture; *Computer Vision and Image Understanding*, 104(2):90–126, 2006.
- [MHK01] Moeslund, T. B., Hilton, A., and Kruger, V.: A survey of advances in vision-based human motion capture and analysis; *Computer Vision and Image Understanding*, 81:231–268, 2001.
- [MMP99] Mascaró, M., Mir, A., and Perales, F.: Visualización de deformaciones dinámicas mediante elementos finitos triangulares y cuadrangulares; In *IX Congreso Español de Informática Gráfica (CEIG'99)*, pages 47–61, June 1999.
- [MSG08] Manohar, V., Shreve, M., Goldgof, D., and Sarkar, S.: Finite element modeling of facial deformation in videos for computing strain pattern; In *Proceedings of the 9th International Conference on Pattern Recognition*, pages 1–4, 2008.
- [MSP<sup>+</sup>09] Maurice, X., Sandholm, A., Pronost, N., Boulic, R., and Thalmann, D.: A subject-specific software solution for the modeling and the visualization of muscles deformation; *The Visual Computer*, 25(9):835–842, 2009.
- [Mur67] Murray, M. P.: Gait as total pattern of movement; *American Journal of Physical Medicine*, 46:290–332, 1967.
- [NDW93] Neider, J., Davis, T., and Woo, M.: *OpenGL Programming Guide* Addison-Wesley Publishing Company, Massachusetts, 1993.
- [NF02] Ng-Thow-Hing, V. and Fiume, E.: Application-specific muscle representation; In *Graphics Interface 2002*, pages 107–116, 2002.
- [NT98] Nedel, L. P. and Thalmann, D.: Real time muscle deformations using mass-spring systems; In Wolter, F.-E. and Patrikalakis, N. M., editors, *Proceedings of the Computer Graphics Interface CGI'98*, pages 156–165, Los Alamitos, California, June 22–26 1998. IEEE Computer Society.
- [OMSA09] Oberhofer, K., Mithraratne, K., Stott, N., and Anderson, I.: Anatomically-based musculoskeletal modeling: prediction and validation of muscle deformation during walking; *The Visual Computer*, 25(9):843–851, 2009.
- [Pau67] Paul, J. P.: Forces transmitted by joints in the human body; In *Proceedings of the Institute of Mechanical Engineering*, volume 181, pages 8–15, 1967.
- [Per01] Perales, F. J.: Human motion analysis and synthesis using computer vision and graphics techniques. state of art and applications; In *Proceedings of the World Multiconference on Systemics, Cybernetics and Informatics*, 2001.
- [Pie95] Pierrynowski, M. R.: *Three-Dimensional Analysis of Human Movement*, chapter 11: Analytic Representation of Muscle Line of Action and Geometry, pages 215–256 Human Kinetics, 1995.
- [RBS02] Rojas, F., Baldassarri, S., and Seron, F.: Software laboratory for physical based human body animation; In Perales, F. and Hancock, E., editors, *Articulated Motion and Deformable Objects*, volume 2492 of *Lecture Notes in Computer Science*, pages 226–240. Springer, 2002.
- [SGMB03] Seron, F., Garcia, E., Magallon, J., and Bosque, A.: Proyecto motrico: Modelado y generación de mallas de arterias coronarias y utilización de algoritmos paralelos en el método de elementos finitos; In Dias, A. M., editor, *CIBEM6: VI Congreso Ibero-Americano de Engenharia Mecânica*, volume I, pages 107–112, 2003.
- [Sok56] Sokolnikoff, I. S.: *Mathematical Theory of Elasticity* Mc Graw-Hill, 1956.

- [SPCM97] Scheepers, F., Parent, R. E., Carlson, W. E., and May, S. F.: Anatomy-based modeling of the human musculature; *Computer Graphics*, 31(Annual Conference Series):163–172, August 1997.
- [SPL<sup>+</sup>05] Sarkar, S., Phillips, P., Liu, Z., Robledo, I., Grother, P., and Bowyer, K.: The humanoid gait challenge problem: Data sets, performance, and analysis; *IEEE Transactions on Pattern Analysis and Machine Intelligence*, 27(2):161–177, 2005.
- [SSK89] Seron, F. J., Sanz, F., and Kindelan, M.: Elastic wave propagation with the finite element method; Technical Report ICE-0028, IBM - European Center for Scientific and Engineering Computing, February 1989.
- [ST95] Shen, J. and Thalmann, D.: Interactive shape design using metaballs and splines; In *Implicit Surfaces'95*, pages 187–196, Grenoble, France, April 1995. Proceedings of the first international workshop on Implicit Surfaces.
- [Ste97] StereoGraphics Corporation: *StereoGraphics developers' handbook* StereoGraphics Corporation, San Rafael, CA, 1997.
- [TBNF03] Teran, J., Blemker, S., Ng-Throw-Hing, V., and Fedkiw, R.: Finite volume methods for the simulation of skeletal muscle; In Breen, D. and Lin, M., editors, *Eurographics/SIGGRAPH Symposium on Computer Animation'03*, pages 68–74, 2003.
- [TSB<sup>+</sup>05] Teran, J., Sifakis, E., Blemker, S., Ng-Thow-Hing, V., Lau, C., and Fedkiw, R.: Creating and simulating skeletal muscle from the visible human data set; *IEEE Transactions on Visualization and Computer Graphics*, 11(3):317–328, May 2005.
- [Ueb97] Ueberhuber, C.: *Numerical Computation 2: Methods, Software, and Analysis* Springer-Verlag, May 1997.
- [VHBH90] Visser, J. J., Hoogkamer, J. E., Bobbert, M. F., and Huijing, P. A.: Length and moment arm of human leg muscles as a function of knee and hip-joint angles; *European Journal of Applied Physiology*, 61:453–460, 1990.
- [VTT<sup>+</sup>06] Viceconti, M., Testi, D., Taddei, F., Martelli, S., Clapworthy, G., and Jan, S.: Biomechanis modeling of the musculoskeletal apparatus: status and key issues; *Proceedings of the IEEE*, 94(4):725–739, April 2006.
- [Whi03] Whittle, M. W.: *Gait Analysis: an introduction* Butterworth-Heinemann, Edinburgh, 3rd edition, 2003.
- [Wil95] Wilhelms, J.: Modeling animals with bones, muscles and skin; Technical Report UCSC-CRL-95-01, University of California, Santa Cruz, Jack Baskin School of Engineering, January 1995.
- [Wil97] Wilhelms, J.: Animals with anatomy; *IEEE Computer Graphics and Applications*, 17(3):22–30, May 1997.
- [Win79] Winter, D. A.: *Biomechanics of Human Movement* Wiley-Interscience. John Wiley & Sons, Inc., New York, 1979.
- [Win87] Winter, D. A.: Mechanical power in human movement: Generation, absorption and transfer; *Med. Sport Sci.*, 35:34–45, 1987.
- [Win90] Winter, D. A.: *Biomechanics and Motor Control of Human Movement* Wiley-Interscience. John Wiley & Sons, Inc., 2nd edition, 1990.
- [WSG<sup>+</sup>98] William, G., Snir, M., Gropp, W., Nitzberg, B., and Lusk, E.: *MPI: The Complete Reference* MIT Press, 1998.
- [WSS<sup>+</sup>09] Wang, H., Sun, S., Shu, T., Shi, F., and Wu, J.: Survey: Parameterized 3d human body modeling and geometric deformation technology; In *Proceedings of IEEE 10th International Conference on Computer Aided Industrial Design*, pages 1486–1493, 2009.
- [WV97] Wilhelms, J. and Van Gelder, A.: Anatomically based modeling; In Whitted, T., editor, *SIGGRAPH 97 Conference Proceedings*, Annual Conference Series, pages 173–180. ACM SIGGRAPH, Addison Wesley, August 1997.

- [YG06] Yesil, M. S. and Gudukbay, U.: Realistic rendering and animation of a multi-layered human body model; In *Proceedings of the Information Visualization (IV'06)*, 2006.
- [ZCK98] Zhu, Q., Chen, Y., and Kaufman, A.: Real-time biomechanically-based muscle volume deformation using FEM; *Computer Graphics Forum*, 17(3):275–284, 1998.
- [ZLW03] Zuo, L., Li, J., and Wang, Z.: Anatomical human musculature modeling for real-time deformation; *Journal of WSCG*, 11, 2003.
- [ZM99] Zheng, Y. and Mak, A.: Effective elastic properties for lower limb soft tissues from manual indentation experiment; *IEEE Transactions on Rehabilitation Engineering*, 7(3):257–267, 1999.
- [ZNK02] Zajac, F. E., Neptune, R. R., and Kautz, S. A.: Biomechanics and muscle coordination of human walking. Part I: Introduction to concepts, power transfer, dynamics and simulations; *Gait and Posture*, 16:215–232, 2002.